Molecular Vision 2004; 10:703-11 <http://www.molvis.org/molvis/v10/a85>
Received 19 August 2004 | Accepted 30 September 2004 | Published 4 October 2004

RNA interference targeting transforming growth factor-β type II receptor suppresses ocular inflammation and fibrosis

Hiroshi Nakamura,[1] Shahid S. Siddiqui,[2] Xiang Shen,[1] Asrar B. Malik,[2] Jose S. Pulido,[1] Nalin M. Kumar,[1] Beatrice Y. J. T. Yue[1]

(The first two authors contributed equally to this publication)

Departments of [1]Ophthalmology and Visual Sciences, and [2]Pharmacology, College of Medicine, University of Illinois at Chicago, Chicago, IL

Purpose: Transforming growth factor-β (TGF-β) is an important mediator of wound healing responses. In the eye, TGF-β activity has been implicated in causing corneal haze after laser surgery and subconjunctival scarring following glaucoma surgery. The purpose of the study was to determine whether small interference RNAs (siRNAs) targeting the type II receptor of TGF-β (TβRII) could be used to suppress the TGF-β action.
Methods: TβRII specific siRNAs designed from the human gene sequence were transfected into cultured human corneal fibroblasts. The protein and transcript levels of the receptor were determined by immunofluorescence, western blotting, and real time PCR. Immunofluorescence and immunoblotting were carried out to examine fibronectin assembly. A wound closure assay was used to assess cell migration in in vitro fibroblast cultures. In addition, the in vivo effects of TβRII siRNA were evaluated in a mouse model of ocular inflammation and fibrosis generated by subconjunctival injection of phosphate buffered saline and latex beads. Mouse TβRII siRNA was introduced into experimental eyes. Cellularity on tissue sections was evaluated after staining with hematoxylin and eosin. Collagen deposition was visualized by picrosirius red staining.
Results: TβRII siRNAs abrogated the receptor transcript and protein expression in cultured corneal fibroblasts. The gene knockdown inhibited fibronectin assembly and retarded cell migration. In the mouse model, introduction of TβRII specific siRNA significantly reduced the inflammatory response and matrix deposition.
Conclusions: TβRII specific siRNAs were efficacious both in vitro and in vivo in knocking down the TGF-β action. A direct application of siRNA into eyes to downregulate TβRII expression may provide a novel therapy for preventing ocular inflammation and scarring.

Transforming growth factor-β (TGF-β), a family of structurally related multifunctional cytokines, has wide biological actions including cell growth, differentiation, apoptosis, and fibrogenesis [1-3]. TGF-β typically is secreted in a latent form and is activated through a complex process of proteolytic activation and dissociation of latency protein subunits [4]. The action of TGF-β is mediated by TGF-β receptors types I (TβRI) and II (TβRII), both of which are serine and threonine kinases. Signal transduction is initiated by TGF-β binding to TβRII, followed by its association with TβRI [4]. TβRII phosphorylates multiple serines and threonines in the TTSGSGSGSG sequence of the cytoplasmic region of TβRI [4]. The activated TβRI in turn phosphorylates and activates the transcription factors, Smads [4,5].

TGF-β has emerged as a key mediator of the fibrotic response to wounding. It is upregulated during different types of wound healing in the eye, liver, and skin [3,6-8]. Of the three human isoforms (TGF-β1, TGF-β2, and TGF-β3), TGF-β2 is the predominant form in the eye [9,10]. TGF-βs have been shown to be important in ocular scarring in conditions including proliferative vitreoretinopathy [11], cataract formation [12], corneal opacities [13], and subconjunctival scarring, a complication of filtration surgery in glaucoma [14,15]. TGF-β also has been implicated in choroidal neovasculaization [16,17].

In glaucoma filtration surgery, postoperative scarring at the wound site is a critical determinant of the surgical outcome [18,19]. Although anti-scarring agents such as mitomycin C and 5-fluorouracil can prevent post-operative scarring and improve surgical outcome [20,21], they do so by causing widespread fibroblast cell death and are associated with severe and potentially blinding complications [22,23]. The important role of TGF-β in the wound repair has led to other strategies [15] such as the use of anti-TGF-β antibody [24,25] and antisense oligonucleotides [26] to block the TGF-β action. These studies have, in general, targeted the ligand rather than the receptor.

In the current study, we used the RNA interference (RNAi) strategy to target the TGF-β pathway. Gene silencing is a process by which double stranded RNA triggers the destruction of mRNAs sharing the same sequence. RNAi is initiated by the conversion of double stranded RNA into 21-23 nucleotide

Correspondence to: Dr. Beatrice Yue, Department of Ophthalmology and Visual Sciences, University of Illinois at Chicago, 1855 West Taylor Street, Chicago, IL, 60612; Phone: (312) 996-6125; FAX: (312) 996-7773; email: Beatyue@uic.edu

fragments, termed small interfering RNAs (siRNAs), that direct the degradation of the target RNAs [27-29]. siRNAs have been shown to be of great value in knocking down genes in a variety of biological systems [30-32].

Since the ligand engagement by TβRII appears to be a major limiting step in cellular activation, we designed siRNAs targeting this receptor. In experiments described herein, the siRNAs induced a marked reduction in the TGF-βmediated matrix deposition and retarded the migration of cultured human corneal fibroblasts. In addition, siRNA specific for TβRII was shown in an in vivo mouse model to reduce inflammation and the complications of wound repair in the eyes.

METHODS

Cell cultures: Normal human corneas from donors aged 13, 29, 34, 45, and 47 years were obtained from the Illinois Eye Bank (Chicago, IL). The procurement of tissues was approved by the Institutional Review Board at the University of Illinois at Chicago in compliance with the declaration of Helsinki. Corneal fibroblasts were derived from the stromas isolated from the corneas. The cells were maintained in serum containing media as previously described [33].

TβRII siRNA sequences: siRNAs were derived from the coding sequence of the human TβRII gene (M85079). The siRNA selection was based on the program at Ambion (Austin, TX), choosing 21 nucleotide sequences that start with AA and have a 30 to 70% GC content. Sequences identified were BLASTed against the Genbank database. Four sequences that cover different regions of the TβRII coding sequence and contain no homology to the non-TβRII sequence were custom synthesized by Dharmacon Research (Lafayette, CO). The target sequences (5' to 3') and the siRNA duplexes for these 4 siRNA duplexes, designated as hT1, hT2, hT3, and hT4, are shown in Table 1, with the position of the first nucleotide in the human TβRII sequence shown in parentheses.

In addition, a nonspecific, scrambled siRNA duplex (Scramble II duplex), used as a control, and a Cy3 labeled luciferase GL2 duplex, used to determine optimal conditions for siRNA transfection, were purchased from Dharmacon. siRNA from the similar region as hT1 of the mouse TβRII sequence (AF406755), was also synthesized and tested for efficacy in vivo in an inflammatory/fibrosis mouse model. The target sequence of the mouse T1 (mT1) siRNA is shown in Table 1. There is one nucleotide difference (small letter) between the human and mouse TβRII sequences.

Table 1. Target and duplex sequences for TβRII specific siRNAs

siRNA duplex	Species	TβRII sequence (5'-3')	siRNA duplex sequences
hT1	Human	(529)AATCCTGCATGAGCAACTGCA	5′UCCUGCAUGAGCAACUGCAdTdT dTdTAGGACGUACUCGUUGACGU
hT2	Human	(1253)AGCATGAGAACATACTCCAG	5′GCAUGAGAACAUACUCCAGdTdT dTdTCGUACUCUUGUAUGAGGUC
hT3	Human	(1113)AAGGCCAAGCTGAAGCAGAAC	5′GGCCAAGCUGAAGCAGAACdTdT dTdTCCGGUUCGACUUCGUCUUG
hT4	Human	(948)AAGACGCGGAAGCTCATGGAG	5′GACGCGGAAGCUCAUGGAGdTdT dTdTCUGCGCCUUCGAGUACCUC
mT1	Mouse	(195)AgTCCTGCATGAGCAACTGCA	5′UCCUGCAUGAGCAACUGCAdTdT dTdCAGGACGUACUCGUUGACGU

Four siRNAs, designated as hT1, hT2, hT3, and hT4, were designed from the coding sequence of the human TβRII gene. The target sequences (5'-3') and the siRNA duplex sequences are listed, with the position of the first nucleotide in the human TβRII sequence shown in parentheses. siRNA from the similar region as hT1 of the mouse TβRII sequence was also designed and the target sequence of the mouse T1 (mT1) siRNA is shown. There is one nucleotide difference (small letter) between the human and mouse TβRII sequences.

Transfection of siRNA duplexes: Normal human corneal fibroblasts were transfected with TβRII specific siRNA duplex (25, 50, 100, or 200 nM final concentration) or scrambled (control) siRNA (100 or 200 nM) using TransIT-TKO reagent (Takara Mirus, Madison, WI), following the manufacturer's protocol. The cells were harvested 16, 24, 48, or 72 h after transfection for analyses. Also as controls, corneal fibroblasts were either untreated or treated only with TransIT-TKO.

Immunofluorescence staining: After transfection, cells were fixed in 2% formaldehyde, permeabilized with 0.1% Triton X-100, and stained with rabbit anti-TβRII antibody (1:100, SC1700; Santa Cruz Biotechnology, Santa Cruz, CA) and FITC conjugated goat anti-rabbit IgG (1:250; Southern Biotechnology, Birmingham, AL). The nuclei of the cells were counterstained with 4',6'-diamidino-2-phenylindole dihydrochloride (DAPI). To observe the fibronectin network, cells were fixed in cold methanol, and immunostained with rabbit anti-human fibronectin (1:100; BD Biosciences, Lexington, KY) and FITC-goat anti-rabbit IgG (1:200; Jackson ImmunoResearch, West Grove, PA).

Western blotting: After siRNA transfection, corneal fibroblasts were lysed in a Triton lysis buffer. Equal amount of protein (20 μg/lane) was resolved on a 10% sodium dodecyl sulfate (SDS)-polyacrylamide gel. The proteins were then transferred to nitrocellulose membranes for probing with rabbit anti-TβRII antibody (1:1000) and horseradish peroxidase (HRP) conjugated goat anti-rabbit IgG (1:5000; Jackson ImmunoResearch). Signals were detected by chemiluminescence and analyzed by densitometry.

For secreted fibronectin, cells (48 h after transfection) were incubated with serum-free media for 24 h. After normalizing against the protein content in cell lysates, equal aliquots of media samples were electrophoresed on 10% SDS polyacrylamide gels under reducing conditions. Immunoblotting was performed using rabbit anti-human fibronectin (1:5000) and HRP-goat anti-rabbit IgG (1:10,000; Jackson ImmunoResearch).

Real time PCR: Total RNA was extracted with Trizol (Invitrogen, Carlsbad, CA) from cells 48 and 72 h after transfection. RNA (100 ng) was converted into cDNA using the Thermoscript RT-PCR system (Invitrogen) with oligo dT and random hexamers.

Primer pairs for the TβRII gene were as described [34]. PCR amplification was performed using a Cepheid SmartCycler. The PCR mixture contained cDNA, Ex Taq R-PCR polymerase (Takara Mirus), 3 mM $MgCl_2$, dNTP, SYBR-Green (Molecular Probes, Portland, OR), and 0.5 μM of each gene specific primer. To normalize samples, real time PCR

reactions containing primers for 18S rRNA (number 1717; Ambion) were also performed. Amplification of PCR products was monitored via intercalation of SYBR-Green. A no template control and a no reverse transcription control were included. Agarose gel electrophoresis was used to verify that the TβRII PCR product was of the correct 75 bp size and that no primer dimers were formed. The C_t values were normalized to 18S rRNA to obtain a mean, normalized TβRII value using the Q-gene software (Version 1) as previously described [35].

Cell migration assay: Corneal fibroblasts after transfection were scratched with a sterile P20 pipet tip [36]. The migration of cells into the wound was examined by phase contrast microscopy 7 h after wounding. Total area of the wound in each 10x field and the area covered by the migrating cells within the wound were measured using an Image Processing Tool Kit (Version 3.0; Reindeer Graphics, Asheville, NC). At least 10 fields were analyzed and the mean percentage of wound area covered by cells was calculated. Student's t test was used for the statistical analysis.

Mouse model of subconjunctival inflammation and fibrosis: The experimental protocol was approved by the animal care committee at the University of Illinois at Chicago. Animal care guidelines comparable to those published by the US Public Health Service were followed. C57BL6 mice underwent general anesthesia with intraperitoneal injections of ketamine and xylazine. The subconjunctival scarring model was generated similar to that reported previously [37], with modifications. Instead of sterile phosphate buffered saline (PBS) alone, 30 µl of PBS containing latex beads (1.053 µm diameter, 300 µg/ml; Polysciences, Warrington, PA) was injected to the temporal subconjunctival space of mouse eyes. For siRNA effects, the left eyes of mice were injected in a masked manner with 30 µl of PBS/beads mixed with 0.1 µl of TransIT-TKO and 200 nM mT1 or scrambled siRNA. To serve as controls, the left eyes of other mice were uninjected, or injected with PBS/latex beads alone or with TransIT-TKO reagent. All the right eyes were untouched. Mice were sacrificed by cervical dislocation 2, 4, 7, and 14 days after injection. At least 4 mice were used for each treatment/time point.

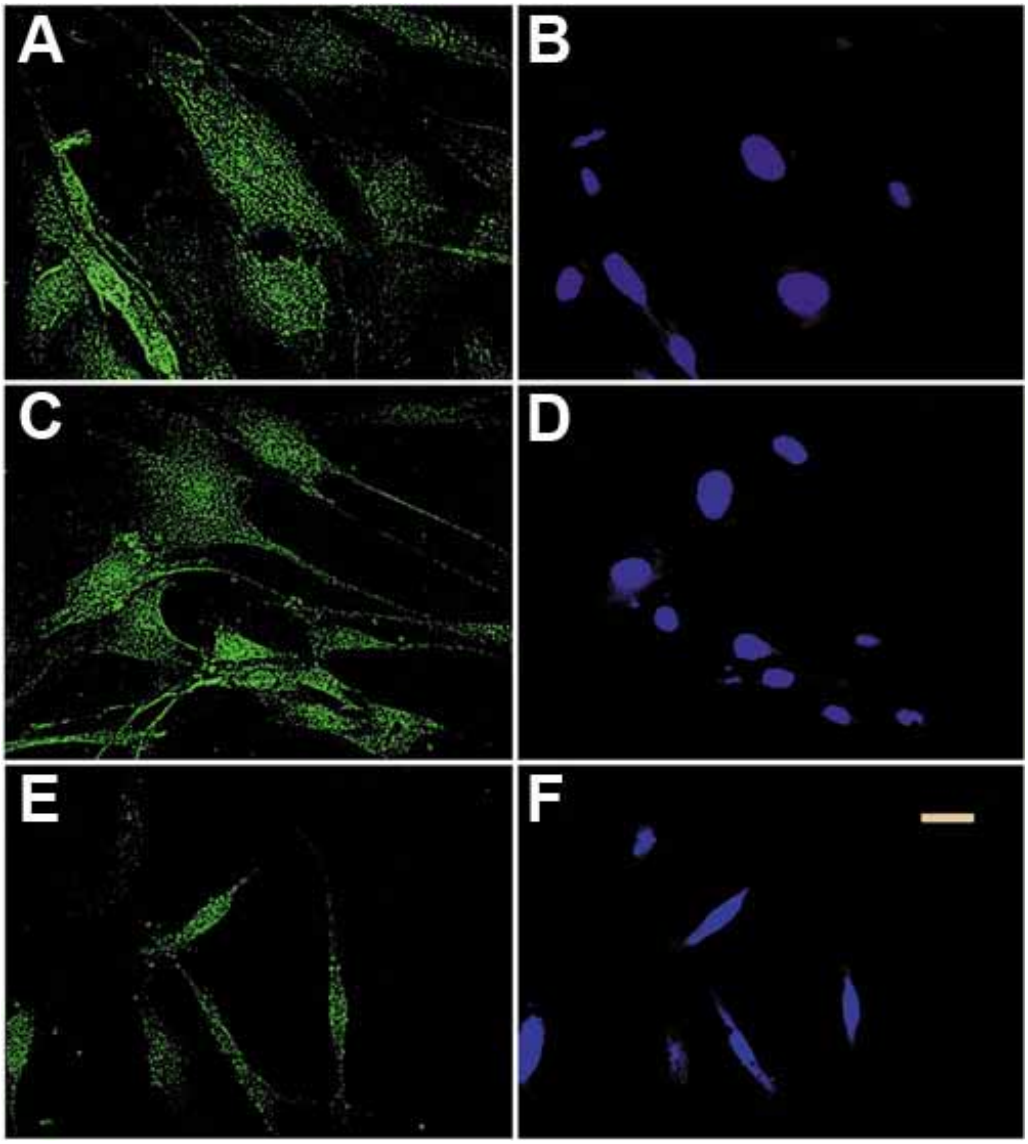

Figure 1. siRNA inhibits TβRII expression. Immunofluorescence analysis of human corneal fibroblasts, untreated (**A**,**B**), treated for 48 h with scrambled siRNA (**C**,**D**), or with 100 nM hT1 (**E**,**F**) was performed. TβRII expression is shown in **A**,**C**, and **E**. Staining of nuclei with DAPI (blue) is shown in **B**, **D**, and **F**. Note the reduction in TβRII staining of cells treated with hT1 siRNA (**E**) compared to control cells (**A**,**C**). The morphology after the siRNA treatment was somewhat altered. The bar represents 10 µm.

Enucleated eyes were fixed with 10% buffered formalin and 5 μm thick paraffin sections were prepared. The sections were stained with hematoxylin and eosin to assess the inflammatory reaction and picrosirius red to demonstrate collagen deposition [37]. The number of inflammatory cells in subconjunctival areas in the sections was counted. The value was normalized to number of inflammatory cells per 2500 μm^2 area underneath the conjunctival epithelium.

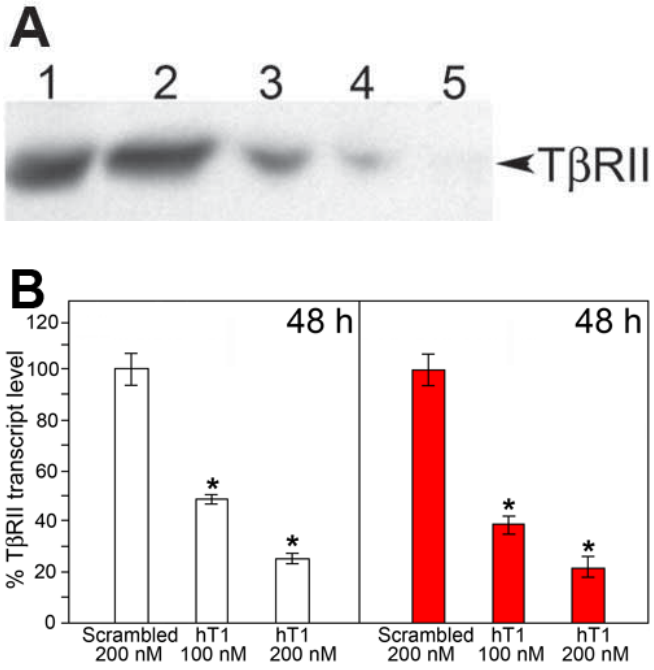

Figure 2. siRNA reduces protein and mRNA levels of TβRII. **A**: siRNAs suppress TβRII protein expression in corneal fibroblasts. Total cell lysates from human corneal fibroblasts treated with hT1 siRNA or control, scrambled siRNA for 48 h were separated on 10% SDS polyacrylamide gels and immunoblotted with a TβRII specific antibody. Lane 1 contains lysate from cells incubated with TransIT-TKO reagent alone (no siRNA). Lane 2 contains lysate from cells treated with 100 nM scrambled siRNA. Lanes 3 and 4 contain lysates of cells treated with hT1 siRNA at a final concentration of 100 nM (lane 3) or 200 nM (lane 4). In lane 5, the TβRII antibody was preincubated with antigenic peptide before probing the normal cell lysate. The TβRII band is indicated. **B**: siRNA reduces levels of TβRII transcript. RNA was prepared from cells treated with scrambled siRNA or hT1 siRNA for 48 or 72 h at either 100 or 200 nM concentration. Following conversion to cDNA, the samples were analyzed by real time PCR using primers to TβRII or 18S rRNA. The bar graphs show the mean expression levels of TβRII transcript normalized to 18S RNA relative to that of scrambled siRNA treated controls. Asterisks indicate that the data are significantly different from the scrambled controls ($p<0.0002$, $n=3$, Student's t test).

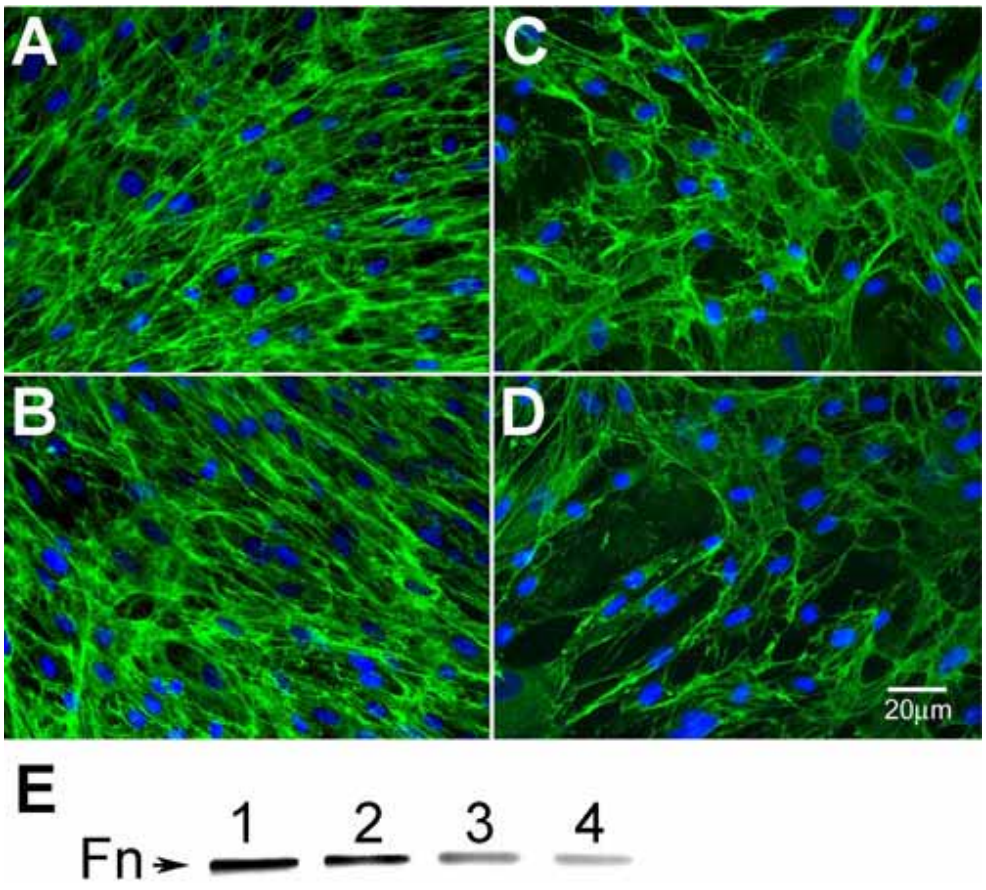

Figure 3. TβRII siRNA interferes with fibronectin production. Immunofluorescence analysis of fibroblasts untreated (**A**), treated for 48 h with scrambled siRNA (**B**), 100 nM hT1 (**C**), or 200 nM hT1 (**D**) was performed to visualize the fibronectin matrix (in green). Nuclei stained with DAPI are seen in blue. **E**: The level of fibronectin secreted to the culture media was analyzed by western blotting. Samples were from cultures untreated (lane 1), treated with scrambled RNA (lane 2), or 100 nM (lane 3) or 200 nM (lane 4) hT1. The fibronectin (Fn) bands are labeled.

RESULTS

Suppression of TβRII protein and mRNA expression: Using the TransIT-TKO reagent, we transfected human corneal fibroblasts with all four siRNAs (hT1-4) designed from the human TβRII gene sequence. The cellular uptake of oligoribonucleotides was initially determined using a Cy3 labeled luciferase siRNA. The transfection was efficient in that greater than 90% of the cells displayed red fluorescence of the luciferase siRNA (data not shown). Immunofluorescence showed punctate staining of TβRII on the surface of untreated control corneal fibroblasts (Figure 1A). The staining was in addition observed in the cytoplasm, particularly in the perinuclear area. When treated with 100 nM hT1 for 48 h, the TβRII staining intensity was markedly reduced (Figure 1E). At 100 nM, hT2, hT3, and hT4 likewise suppressed the TβRII staining intensity (data not shown). The inhibitory effect was also observed to varying degrees for all four siRNAs with other concentrations (50 and 200 nM) and time points (24 and 72 h). This response however was not evident at the lowest concentration (25 nM) and the shortest time point (16 h) tested. Overall, hT1 and hT2 resulted in a greater inhibition than hT3 and hT4. Cells treated with scrambled siRNA (Figure 1C) exhibited a similar staining intensity and pattern as the untreated control cells (Figure 1A).

Western blotting (Figure 2A) yielded a 73-75 kDa band immunoreactive to anti-TβRII in the vehicle treated control and scrambled siRNA transfected samples. The protein band was diffuse as TβRII is a glycoprotein. At 48 h, 100 and 200 nM hT1 siRNA induced a marked decrease in signal intensity for TβRII compared to vehicle or scrambled RNA treated controls. Densitometric analysis indicated a 70-85% reduction of TβRII expression in the siRNA treated samples. When the TβRII antibody was preincubated with the antigenic peptide before probing, the immunoreactive band disappeared (Figure 2A, lane 5) confirming the specificity of the antibody.

TβRII transcript levels were examined by real time PCR using 18S rRNA to normalize the data. Figure 2B shows the mean normalized TβRII gene expression as determined by the method of Muller et al [35]. Compared to scrambled siRNA, hT1 at 100 and 200 nM reduced ($p<0.0002$) the level of TβRII transcripts at both 48 and 72 h time points. There was also a dose dependent response as the 200 nM concentration was more effective than 100 nM.

TβRII siRNA impairs fibronectin assembly and fibronectin secretion: Visualized by immunofluorescence, untreated control and scrambled siRNA treated corneal fibroblasts exhibited robust fibronectin deposition and a dense fibrillar network over cells (Figure 3A,B). The fibronectin deposition was clearly reduced in cells 48 h after transfection with both 100 and 200 nM of hT1 siRNA (Figure 3C,D). Cell density was similar in the various specimens and thus the decreased fibronectin assembly was not related to reduction in cell number.

Western blotting was carried out to determine whether the effect of siRNAs on the fibronectin fibrillogenesis was a reflection of decreased fibronectin secretion. Corneal fibroblasts, 48 h after transfection, were incubated in serum-free medium for 24 h. Proteins in the media were subjected to electrophoresis and immunoblotting (Figure 3E). A 220 kDa fibronectin band was observed in all samples. Consistent with

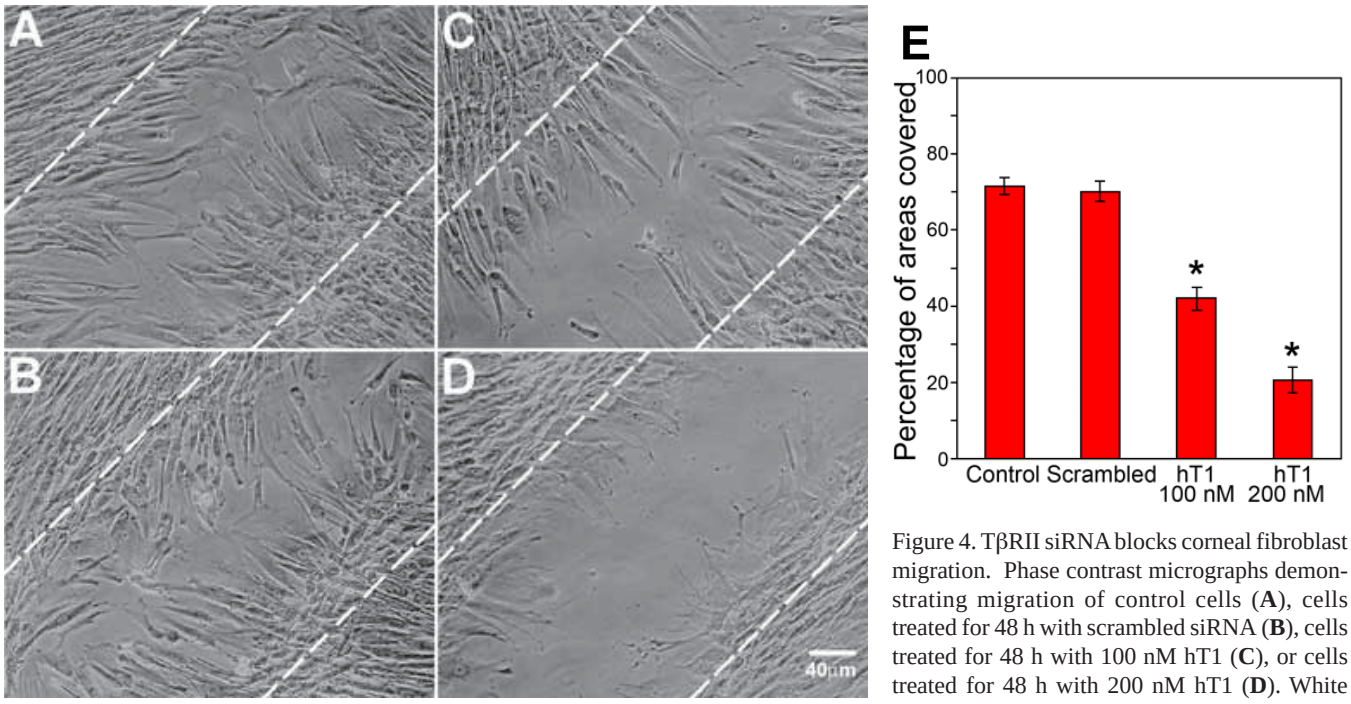

Figure 4. TβRII siRNA blocks corneal fibroblast migration. Phase contrast micrographs demonstrating migration of control cells (**A**), cells treated for 48 h with scrambled siRNA (**B**), cells treated for 48 h with 100 nM hT1 (**C**), or cells treated for 48 h with 200 nM hT1 (**D**). White dotted lines mark the wound edges. **E**: Bar graph showing mean percentage of wound area covered by migrating corneal fibroblasts in each specimen (n=10); error bars represent the standard error of the mean. Asterisks denote values significantly different from those of scrambled RNA treated controls ($p<0.0001$). Experiments were repeated 3 times, yielding similar results.

the immunofluorescence data, treatment with 100 nM hT1 (Figure 3E, lane 3) and 200 nM hT1 (Figure 3E, lane 4) resulted in decreased fibronectin secretion into the culture media. The siRNA elicited a greater effect with 200 (66% reduction compared to the scrambled siRNA treated sample) than 100 nM (40% reduction).

TβRII siRNA blocks corneal fibroblast migration: Wound scratch assays indicated that corneal fibroblasts migrated into the wounded area (Figure 4A). Within 7 h, untreated control and scrambled RNA transfected cells filled 71.8±4.3% and 69.3±5.8% of the pipette tip generated wound area (Figure 4E), respectively. By contrast, the percent wound area covered by 100 nM hT1 (42.3±10.2%) and 200 nM hT1 (21.9±3.9%) transfected cells was significantly decreased ($p<0.0001$).

TβRII siRNA markedly reduces ocular inflammation and fibrosis in a mouse model: To generate a mouse model of inflammation and fibrosis, PBS and latex beads were injected

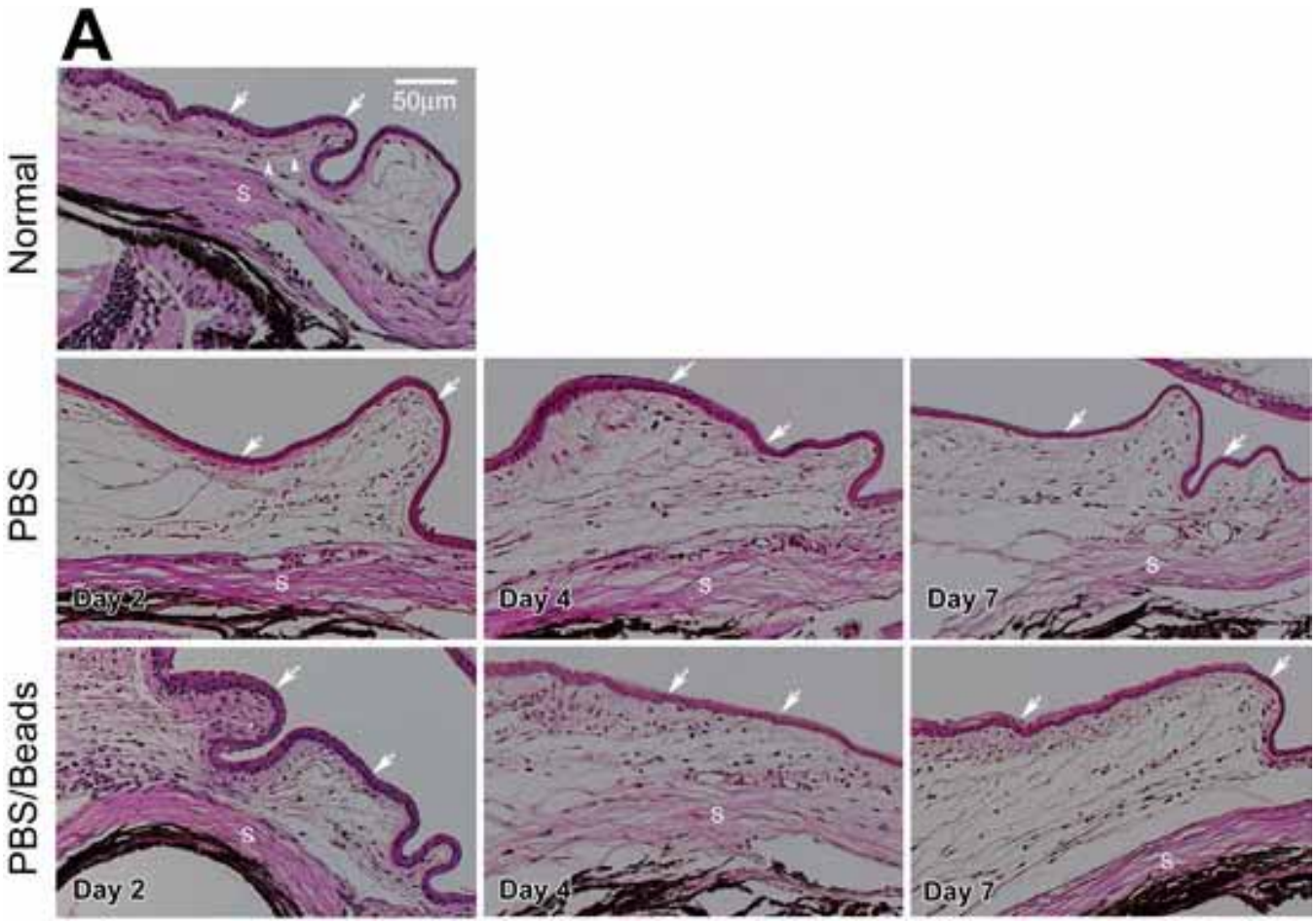

Figure 5. Inflammatory response in mouse models. **A**: Tissue sections from a normal mouse eye. An eye injected with PBS alone, and an eye injected with PBS mixed with latex beads was stained with hematoxylin and eosin to assess cellularity. Note the long, spindle shaped fibroblasts (arrowheads) underneath the conjunctival epithelium (arrows) in the normal mouse eye. Infiltration of the large, round inflammatory cells was observed in mouse eyes 2, 4, and 7 days after injection with either PBS alone or with PBS/beads. The S indicates the sclera. The bar represents 50 µm. **B**: Bar graph showing the number of inflammatory cells per 2,500 μm^2 of subconjunctival area in eyes 2, 4, and 7 days after being injected with PBS alone or with PBS/beads. The data are presented as means (n=8 for day 2 and n=4 for days 4 and 7); error bars represent the standard error of the mean. Asterisks indicate values significantly different from those in PBS injected eyes ($p<0.011$).

into the subconjunctival space of mice. A model has been described previously using only PBS for injections [37], in which the inflammatory response was observed between days 1 and 3 and collagen deposition was seen on day 14 following injections. In the PBS/beads model, round and large inflammatory cells (Figure 5A), contrasting the long, spindle shaped fibroblasts (Figure 5A, arrowheads), were observed after hematoxylin and eosin staining in the subconjunctival space within 2 days of injection. The number of inflammatory cells per 2,500 μm^2 area underneath the conjunctival epithelium was significantly greater ($p<0.011$) in the PBS/latex beads injected eyes than with PBS alone (Figure 5B). The inflammatory response observed on day 2 subsided on days 4 and 7 (Figure 5A,B). Since subconjunctival injection of PBS/beads augmented the inflammatory response, this model was used to test the siRNA effects.

siRNA with mouse sequences corresponding to those of hT1 (designated as mT1), or scrambled siRNA was introduced into mouse eyes together with PBS/latex beads in a masked manner. Two days following the injection, numerous inflammatory cells were observed underneath the conjunctival epithelium in the scrambled RNA treated and PBS/latex beads injected control eyes. In comparison, the infiltration of inflammatory cells was significantly less ($p<0.015$) in mT1 treated eyes (Figure 6A,B). On post-injection day 14, picrosirius red staining showed thick collagen deposition underneath the conjunctival epithelium of scrambled RNA treated eyes (Figure 6C). The fibrotic response was markedly repressed by treatment with mT1 siRNA (Figure 6C).

DISCUSSION

The present study demonstrates that siRNAs specific to human TβRII knocked down the receptor expression in cultured human corneal fibroblasts. Immunofluorescence staining, western blotting, and real time PCR analyses showed the effectiveness of the dose and time dependent inhibition; that is, at concentrations ranging from 25 to 200 nM and time points from 16 to 72 h. We showed that two (hT1 and hT2) of the four siRNAs tested were more efficacious. The confidence of the data is established since gene silencing is produced from siRNAs designed from different regions of the TβRII gene.

Corneal fibroblasts constitutively express TGF-β [38], which induces the expression of matrix molecules such as fibronectin and collagen type I [38,39] and facilitates the mi-

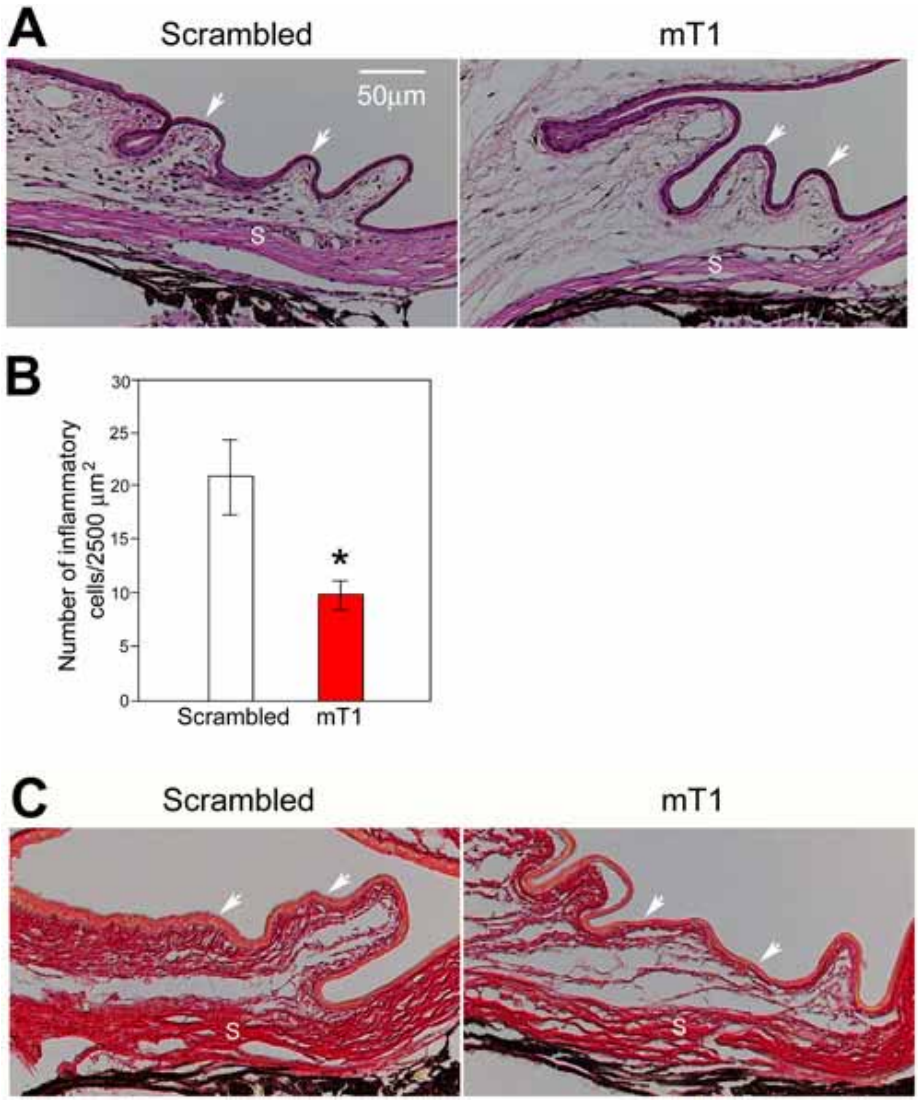

Figure 6. Suppression of inflammatory response and collagen deposition by TβRII siRNA. **A**: Hematoxylin and eosin stained tissue sections from mouse eyes 2 days after injection with PBS/latex beads along with 200 nM scrambled or mT1 siRNA. Arrows indicate the conjunctiva and S indicates the sclera. The bar represents 50 μm. **B**: Bar graph showing the number of inflammatory cells per 2,500 μm^2 of subconjunctival area in eyes injected with 200 nM of mT1 compared to those treated with scrambled siRNA. Data are presented as means (n=5); error bars represent the standard error of the mean. The asterisk indicates values significantly different from those of scrambled RNA treated controls ($p<0.015$). **C**: Tissue sections from eyes 14 days after injection were stained with picrosirius red to demonstrate deposition of collagen that appears as pink fibrillar structures. Note the thick subconjunctival collagen layers in the scrambled siRNA treated mouse eye. Arrows indicate the conjunctival epithelium and S indicates the sclera.

gration of corneal fibroblasts [39,40]. Both of these are critical steps in the wound repair process [41]. In the current study, we showed that fibronectin secretion and deposition were reduced and corneal fibroblast migration was markedly retarded with the siRNA treatment. These findings are consistent with the disruption of the TGF-β signaling pathway by the siRNA directed against TβRII.

The siRNA effect was also demonstrated in a mouse model of ocular inflammation and fibrosis. Our model is similar to that described by Reichel, et al. [37], but instead of injecting PBS alone into the subconjunctival space, we injected PBS mixed with latex beads into mouse eyes. This resulted in a marked augmentation of the inflammatory response. Even in this severe inflammatory model, we observed that mT1 siRNA at 200 nM was effective in blocking the inflammatory and fibrotic responses in the mouse eyes. The reduced fibrosis may be related to the reduced inflammation, impeded fibroblast migration, or diminished matrix deposition. It is also noteworthy that while adenovirus and other vectors may be employed for long term inhibition of inflammation, transient knockdown by synthetic siRNAs allows a better dosage control and may minimize potential side effects. Certainly in our mouse model, a one-time administration of siRNA at a very early phase was sufficient to control the inflammatory process.

Ocular fibrotic wound response is a major cause of impaired vision and blindness, especially following surgical treatment for glaucoma [18,19]. Excessive post-operative scarring often leads to failure of filtration surgery. While the use of antimetabolites such as mitomycin C and 5-fluorouracil as conjunctival anti-scarring treatments benefits a number of patients, these agents are associated with potentially blinding complications including hypotony, maculopathy, and infection [20-23]. Therefore, sequestering of mature TGF-β is an important target in preventing inflammation and fibrosis. Antibodies to TGF-β2 have been reported to reduce conjunctival scarring [24,25]. In addition, antisense oligonucleotides [26,42] or ribozymes [43] to TGF-β were shown to be effective in wound healing in animal and cell culture studies. However, the neutralizing antibody approach exhibits relatively weak effects in general as it may not gain full access to the targeted TGF-β molecules [43]. Antisense phosphorothioate oligonucleotides and ribozymes can be successful, but their effectiveness [44], stability, and specificity are still in debate. The concentrations needed are also generally in the μM range, whereas as the present study indicates, the mT1 siRNA is efficacious at 200 nM. Additionally, our approach of targeting the TGF-β receptor [45] rather than the ligand allows for more specific and effective knockdown of the cytokine function.

In summary, the current study demonstrates that downregulation of the TβRII gene by local application of siRNA prevents ocular inflammation and fibrosis. Our results underscore the potential of a novel therapy for preventing the inflammatory response and scarring in ocular diseases and after glaucoma filtration surgery. This approach may also have applications for other surface tissues, including the skin.

DISCLOSURE

Shahid S. Siddiqui, Asrar B. Malik, Jose S. Pulido, Nalin M. Kumar, and Beatrice Y. J. T. Yue have filed a patent application based on the work described in this manuscript.

ACKNOWLEDGEMENTS

The authors thank Stanley Moskal, Hiroshi Sakai, Haripriya Rajmani, and Yaseen Khan for technical assistance. This work was supported by grant EY03890 (BYJTY), EY05628 (BYJTY), EY013605 (NMK), HL 64573 (ABM), and core grant EY01792 from the National Institutes of Health, Bethesda, MD, and by an unrestricted grant from Research to Prevent Blindness, New York, NY.

REFERENCES

1. Massague J, Cheifetz S, Laiho M, Ralph DA, Weis FM, Zentella A. Transforming growth factor-beta. Cancer Surv 1992; 12:81-103.
2. Piek E, Heldin CH, Ten Dijke P. Specificity, diversity, and regulation in TGF-beta superfamily signaling. FASEB J 1999; 13:2105-24.
3. Border WA, Noble NA. Transforming growth factor beta in tissue fibrosis. N Engl J Med 1994; 331:1286-92.
4. Massague J. TGF-beta signal transduction. Annu Rev Biochem 1998; 67:753-91.
5. Massague J. How cells read TGF-beta signals. Nat Rev Mol Cell Biol 2000; 1:169-78.
6. Connor TB Jr, Roberts AB, Sporn MB, Danielpour D, Dart LL, Michels RG, de Bustros S, Enger C, Kato H, Lansing M, Hayashi, H, glaser BM. Correlation of fibrosis and transforming growth factor-beta type 2 levels in the eye. J Clin Invest 1989; 83:1661-6.
7. McCormick LL, Zhang Y, Tootell E, Gilliam AC. Anti-TGF-beta treatment prevents skin and lung fibrosis in murine scleroderma graft-versus-host disease: a model for human scleroderma. J Immunol 1999; 163:5693-9.
8. Shah M, Foreman DM, Ferguson MW. Neutralisation of TGF-beta 1 and TGF-beta 2 or exogenous addition of TGF-beta 3 to cutaneous rat wounds reduces scarring. J Cell Sci 1995; 108 (Pt 3):985-1002.
9. Lutty GA, Merges C, Threlkeld AB, Crone S, McLeod DS. Heterogeneity in localization of isoforms of TGF-beta in human retina, vitreous, and choroid. Invest Ophthalmol Vis Sci 1993; 34:477-87.
10. Pasquale LR, Dorman-Pease ME, Lutty GA, Quigley HA, Jampel HD. Immunolocalization of TGF-beta 1, TGF-beta 2, and TGF-beta 3 in the anterior segment of the human eye. Invest Ophthalmol Vis Sci 1993; 34:23-30.
11. Kon CH, Occleston NL, Aylward GW, Khaw PT. Expression of vitreous cytokines in proliferative vitreoretinopathy: a prospective study. Invest Ophthalmol Vis Sci 1999; 40:705-12.
12. Hales AM, Chamberlain CG, McAvoy JW. Cataract induction in lenses cultured with transforming growth factor-beta. Invest Ophthalmol Vis Sci 1995; 36:1709-13.
13. Chen C, Michelini-Norris B, Stevens S, Rowsey J, Ren X, Goldstein M, Schultz G. Measurement of mRNAs for TGFβ and extracellular matrix proteins in corneas of rats after PRK. Invest Ophthalmol Vis Sci 2000; 41:4108-16.
14. Cordeiro MF. Role of transforming growth factor beta in conjunctival scarring. Clin Sci (Lond) 2003; 104:181-7. Erratum in: Clin Sci (Lond). 2003; 105:723.

15. Cordeiro MF. Beyond Mitomycin: TGF-beta and wound healing. Prog Retin Eye Res 2002; 21:75-89.
16. He S, Jin ML, Worpel V, Hinton DR. A role for connective tissue growth factor in the pathogenesis of choroidal neovascularization. Arch Ophthalmol 2003; 121:1283-8.
17. Yamanaka R, Ogata N, Yamamoto C, Matsushita M, Matsuzaki K, Uyama M, Matsumura M. Expression of transforming growth factor-beta receptors in normal rat retina and experimental choroidal neovascularization. Jpn J Ophthalmol 2002; 46:525-32.
18. Migdal C, Gregory W, Hitchings R. Long-term functional outcome after early surgery compared with laser and medicine in open-angle glaucoma. Ophthalmology 1994; 101:1651-6; discussion1657.
19. Addicks EM, Quigley HA, Green WR, Robin AL. Histologic characteristics of filtering blebs in glaucomatous eyes. Arch Ophthalmol 1983; 101:795-8.
20. Khaw PT, Doyle JW, Sherwood MB, Grierson I, Schultz G, McGorray S. Prolonged localized tissue effects from 5-minute exposures to fluorouracil and mitomycin C. Arch Ophthalmol 1993; 111:263-7.
21. Cordeiro MF, Reichel MB, Gay JA, D'Esposita F, Alexander RA, Khaw PT. Transforming growth factor-beta1, -beta2, and -beta3 in vivo: effects on normal and mitomycin C-modulated conjunctival scarring. Invest Ophthalmol Vis Sci 1999; 40:1975-82.
22. Crowston JG, Akbar AN, Constable PH, Occleston NL, Daniels JT, Khaw PT. Antimetabolite-induced apoptosis in Tenon's capsule fibroblasts. Invest Ophthalmol Vis Sci 1998; 39:449-54.
23. Stamper RL, McMenemy MG, Lieberman MF. Hypotonous maculopathy after trabeculectomy with subconjunctival 5-fluorouracil. Am J Ophthalmol 1992; 114:544-53.
24. Cordeiro MF, Gay JA, Khaw PT. Human anti-transforming growth factor-beta2 antibody: a new glaucoma anti-scarring agent. Invest Ophthalmol Vis Sci 1999; 40:2225-34.
25. Mead AL, Wong TT, Cordeiro MF, Anderson IK, Khaw PT. Evaluation of anti-TGF-beta2 antibody as a new postoperative anti-scarring agent in glaucoma surgery. Invest Ophthalmol Vis Sci 2003; 44:3394-401.
26. Cordeiro MF, Mead A, Ali RR, Alexander RA, Murray S, Chen C, York-Defalco C, Dean NM, Schultz GS, Khaw PT. Novel antisense oligonucleotides targeting TGF-beta inhibit in vivo scarring and improve surgical outcome. Gene Ther 2003; 10:59-71.
27. Elbashir SM, Harborth J, Lendeckel W, Yalcin A, Weber K, Tuschl T. Duplexes of 21-nucleotide RNAs mediate RNA interference in cultured mammalian cells. Nature 2001; 411:494-8.
28. Fire A, Xu S, Montgomery MK, Kostas SA, Driver SE, Mello CC. Potent and specific genetic interference by double-stranded RNA in Caenorhabditis elegans. Nature 1998; 391:806-11.
29. Hannon GJ. RNA interference. Nature 2002; 418:244-51.
30. Reich SJ, Fosnot J, Kuroki A, Tang W, Yang X, Maguire AM, Bennett J, Tolentino MJ. Small interfering RNA (siRNA) targeting VEGF effectively inhibits ocular neovascularization in a mouse model. Mol Vis 2003; 9:210-6 .
31. Song E, Lee SK, Wang J, Ince N, Ouyang N, Min J, Chen J, Shankar P, Lieberman J. RNA interference targeting Fas protects mice from fulminant hepatitis. Nat Med 2003; 9:347-51.
32. Dykxhoorn DM, Novina CD, Sharp PA. Killing the messenger: short RNAs that silence gene expression. Nat Rev Mol Cell Biol 2003; 4:457-67.
33. Yue BY, Baum JL. Studies of corneas in vivo and in vitro. Vision Res 1981; 21:41-3.
34. Huang C, Kim Y, Caramori ML, Fish AJ, Rich SS, Miller ME, Russell GB, Mauer M. Cellular basis of diabetic nephropathy: II. The transforming growth factor-beta system and diabetic nephropathy lesions in type 1 diabetes. Diabetes 2002; 51:3577-81.
35. Muller PY, Janovjak H, Miserez AR, Dobbie Z. Processing of gene expression data generated by quantitative real-time RT-PCR. Biotechniques 2002; 32:1372-4,1376,1378-9. Erratum in: Biotechniques. 2002; 33:514.
36. Mostafavi-Pour Z, Askari JA, Parkinson SJ, Parker PJ, Ng TT, Humphries MJ. Integrin-specific signaling pathways controlling focal adhesion formation and cell migration. J Cell Biol 2003; 161:155-67.
37. Reichel MB, Cordeiro MF, Alexander RA, Cree IA, Bhattacharya SS, Khaw PT. New model of conjunctival scarring in the mouse eye. Br J Ophthalmol 1998; 82:1072-7.
38. Song QH, Singh RP, Richardson TP, Nugent MA, Trinkaus-Randall V. Transforming growth factor-beta1 expression in cultured corneal fibroblasts in response to injury. J Cell Biochem 2000; 77:186-99.
39. Massague J. The transforming growth factor-beta family. Annu Rev Cell Biol 1990; 6:597-641.
40. Andresen JL, Ledet T, Ehlers N. Keratocyte migration and peptide growth factors: the effect of PDGF, bFGF, EGF, IGF-I, aFGF and TGF-beta on human keratocyte migration in a collagen gel. Curr Eye Res 1997; 16:605-13.
41. Clark RAF. Cutaneous wound repair. In: Goldsmith LA, editor. Physiology, Biochemistry, and Molecular biology of the Skin. 2nd ed. New York: Oxford University Press; 1991. p. 576-601.
42. Shen ZJ, Kim SK, Kwon OS, Lee YS, Moon BJ. Specific inhibition of transforming growth factor-beta2 expression in human osteoblast cells by antisense phosphorothioate oligonucleotides. Eur J Biochem 2001; 268:2331-7.
43. Yamamoto K, Morishita R, Tomita N, Shimozato T, Nakagami H, Kikuchi A, Aoki M, Higaki J, Kaneda Y, Ogihara T. Ribozyme oligonucleotides against transforming growth factor-beta inhibited neointimal formation after vascular injury in rat model: potential application of ribozyme strategy to treat cardiovascular disease. Circulation 2000; 102:1308-14.
44. Stein CA. The experimental use of antisense oligonucleotides: a guide for the perplexed. J Clin Invest 2001; 108:641-4.
45. Shi Y, Massague J. Mechanisms of TGF-beta signaling from cell membrane to the nucleus. Cell 2003; 113:685-700.

The print version of this article was created on 4 Oct 2004. This reflects all typographical corrections and errata to the article through that date. Details of any changes may be found in the online version of the article.